Remote sensing of cropping practice in Northern Italy using time-series from Sentinel-2

Thor-Bjørn Ottosen[a,*], Suzanne T.E. Lommen[b], Carsten Ambelas Skjøth[a]

[a] School of Science and the Environment, University of Worcester, Henwick Grove, WR2 6AJ Worcester, United Kingdom
[b] Department of Biology, University of Fribourg, Chemin du Musée 10, 1700 Fribourg, Switzerland

ARTICLE INFO

Keywords:
NDVI
Time-series analysis
Clustering
Phenology
Weed infestation

ABSTRACT

Maps of cropping practice, including the level of weed infestation, are useful planning tools e.g. for the assessment of the environmental impact of the crops, and Northern Italy is an important example due to the large and diverse agricultural production and the high weed infestation. Sentinel-2A is a new satellite with a high spatial and temporal resolution which potentially allows the creation of detailed maps of cropping practice including weed infestation. To explore the applicability of Sentinel-2A for mapping cropping practice, we analysed the Normalised Differential Vegetation Index (NDVI) time series from five weed-infested crop fields as well as the areas designated as non-irrigated agricultural land in Corine Land Cover, which also contributed to an increased understanding of the cropping practice in the region. The analysis of the case studies showed that the temporal resolution of Sentinel-2A was high enough to distinguish the gross features of the cropping practice, and that high weed infestations can be detected at this spatial resolution. The analysis of the entire region showed the potential for mapping cropping practice using Sentinel-2. In conclusion, Sentinel-2A is to some extent applicable for mapping cropping practice with reasonable thematic accuracy.

1. Introduction

Precise information about the cropping practice in a specific region is important for a range of scientific and planning purposes including assessing the environmental consequences of the crops (Leff et al., 2004). In the following a cropping practice is defined in line with Bégué et al. (2018) as the “planting arrangement in time and space on a piece of land, and associated crop management techniques”. One commonly applied approach to obtain this information is through satellite remote sensing.

Satellite remote sensing has been used in agriculture since the first Landsat satellite in the 1970s. Compared to ground surveys or questionnaires, remote sensing has the advantage to be able to quickly cover a large area, monitor temporal changes and require less manual labour. In recent years, in line with increasing computer power, agricultural mapping approaches have progressed from single image towards multi-temporal approaches using satellites such as AVHRR (e.g. Jakubauskas et al. (2002)), MODIS (e.g. Estel et al. (2016)), and SPOT VEGETATION (Nguyen et al., 2012). This has spurred a development towards increasingly detailed agricultural maps moving from traditional land cover maps towards maps of cropping practice (Bégué et al., 2018). One commonly applied method is using time series of vegetation indices as input to the classification, which has been applied in e.g. China (Chen et al. (2014), Zhang et al. (2008)), Vietnam (Nguyen et al., 2012), USA (Zhang and Hepner, 2017), and Northern Italy (Villa et al., 2015).

Northern Italy, the Po Valley in particular, is one of the few regions in Europe with a consistent high agricultural production in a large number of sectors such as cereals, vegetables, wine, poultry and associated animal production (e.g. Olsen (2010)).

Villa et al. (2015) mapped seven crop types, using Landsat 8 and COSMO-SkyMed, in Northern Italy in near real-time for mid-season and showed an improved thematic accuracy when combining radar satellite data with optical satellite data.

Weeds are a major agricultural problem causing an estimated 34% of global crop losses (Oerke, 2006). Some agricultural weeds; such as common common ragweed, *Ambrosia artemisiifolia L.* common ragweed constitute invasive species and also have negative impact on the public health (e.g. Smith et al. (2013)). Knowledge of the spatial and temporal distribution of such weeds is therefore essential to better monitor their spread and to target areas for management (Latombe et al., 2017). Northern Italy is characterized by high densities of common ragweed (Smith et al., 2013) especially on stubble fields after the harvest of cereals typically early July (e.g. Lehoczky et al. (2013)). The high temporal and spatial variability of this phenomenon makes remote

* Corresponding author.
E-mail address: Suzannelommen@hotmail.com (S.T.E. Lommen).

sensing a natural choice of study method. This region is also largely affected by Johnson grass (Sorghum halepense) and velvetleaf (Abutilon theophrasti) (Francesco Vidotto, personal communication). Mapping cropping practice, including weed infestation, is expected to improve mitigation of weeds including common ragweed.

Remote sensing of weed infestation has hitherto been hampered by the small size and patchiness (Müllerová et al., 2017). For common ragweed, Ngom and Gosselin (2014) mapped the likelihood of common ragweed presence in Quebec, Canada and Auda et al. (2008a) mapped the common ragweed cover in the Rhone-Alpes region of France. Rakotoniaina et al. (2009) compared two methods for mapping common ragweed and Auda et al. (2008b) applied a non-parametric classification, founded on the maximum likelihood classification, to multi-temporal images. Studies on other weeds are rather scarce. Most of these studies used a classification approach based on a single image (or a few closely dated images). Identifying specific herbaceous plants, from single images is a challenge, however, due to the difficulty to distinguish them from other vegetation (Laba et al., 2005, Müllerová et al., 2017), and the possibility of using a time series approach for detection has thus received less attention.

The Sentinel-2A satellite was launched in 2015 and has a spatial resolution (in four bands) of up to 10 m × 10 m and a temporal resolution of approximately 10 days (Drusch et al., 2012). The spatial resolution is thus higher than satellites such as MODIS and SPOT VEGETATION, at the expense of a lower temporal resolution. Given that this is a new satellite, the sufficiency of the spatial and temporal resolution of this satellite for mapping cropping practice, including weed infestation, has yet to be determined.

To explore the applicability of Sentinel-2A for mapping cropping practice, we first analysed the Normalised Differential Vegetation Index (NDVI) time series from five crop fields, infested with common ragweed, in Northern Italy, using in situ observations and the corresponding RGB (red, green, blue) images from Sentinel-2. Subsequently, to form a better view of the cropping practice in Northern Italy, and at the same time gain further insight into the applicability of Sentinel-2 for mapping cropping practice; we classified the time series from Sentinel-2 for the entire region, and assessed the accuracy of the resulting land cover map.

2. Methods

2.1. Study area

The study area, mainly located in the Piedmont region of Italy include parts of the Italian Po plain, which is mostly flat and intensively cultivated. The two Sentinel-2 tiles (T32TMR and T32TLQ, Fig. 1) cover a total area of $2.38 \cdot 10^4$ km^2. The administrative centre is the city of Turin and according to Harris et al. (2014), the annual mean temperature is 12.3 °C with monthly means varying from 2.2 °C in the winter to 22.1 °C in the summer. The annual precipitation is 1016 mm, peaking in late spring and autumn and with a relatively dry winter period (40–50 mm/month) within the months December-February. According to Eurostat (http://ec.europa.eu/eurostat/web/agriculture/data/database) (2013 numbers, tables named ef_mainfarm and ef_landuse), the agricultural land is mainly used for permanent grassland (38%), permanent crops (9%) and cereals (40%). Minor crops including legumes, root crops and industrial crops account for 10% of the area. The cereals are dominated by common wheat (9%), barley (1%), maize (17%) and rice (12%) (all percentages are of total area). The distribution between spring crops and winter crops is, according to Leff et al. (2004), generally not recorded systematically and thus not part of the Eurostat databases. However, Leff et al. (2004) also records, that the main wheat variety in Europe is winter wheat with a typical harvest time in June-August, while maize is considered a spring crop with a later harvest time. Barley, a minor crop in this region, is in Europe used both as a spring crop and as a winter crop.

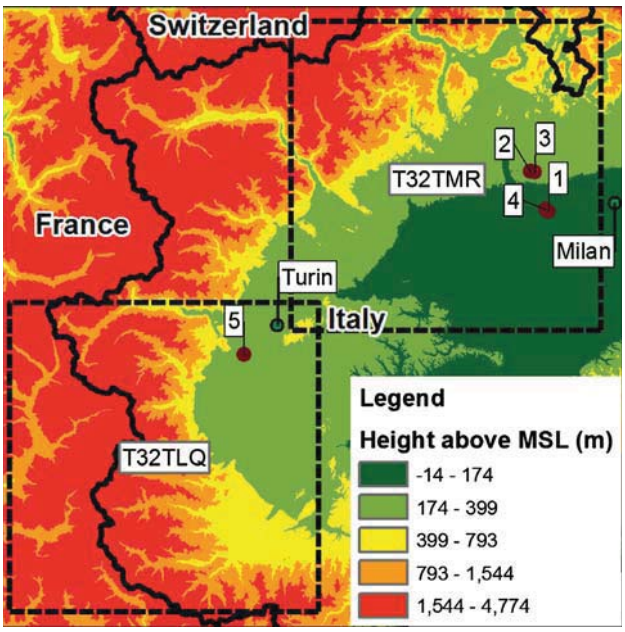

Fig. 1. Map of the two Sentinel-2 tiles and the five case study sites. Numbers correspond to the numbers in Table 1. Cities are marked as the city centre. The colours represent height above mean sea level (MSL). Country boundaries and cities source: Esri (www.arcgis.com), elevation: Reuter et al., (2007).

2.2. Selection of case studies

Common ragweed, originating from North America, is one of the important weeds in the area. It was first recorded in the west of Piedmont in 1902 (Ciappetta et al., 2016) and then spread across the entire Po Plain. In Piedmont, local authorities promote the management of common ragweed before the end of August, when it emits highly allergenic pollen adversely affecting human health. Non-grassy weeds are commonly suppressed during cropping by the use of general herbicides acting against non-grasses. Although common ragweed is a non-grassy weed, it is hard to completely eliminate due to its large capacity for regrowth after the application of herbicides (Sölter et al., 2016). Moreover, due to its long germination period, it can still germinate later in summer (Kazinczi et al., 2008) and then quickly grow when competition from cereals is eliminated by the harvest. This can result in near-monocultures of common ragweed with high density sometimes resulting in a carpet-like cover (Lehoczky et al., 2013). Typically, the fields remain unused until sowing in late autumn (pers. comm. Francesco Vidotto). Since a few years common ragweed in this area is also heavily attacked by the ragweed leaf beetle, *Ophraella communa*. This is a natural enemy from the native range of the plant that is thought to have been accidentally introduced into Europe (Müller-Schärer et al., 2014). Defoliation of the plants typically increases rapidly in the second half of August turning green plants brown within one to two weeks (personal observation Lommen et al.).

Within the two tiles, we selected five stubble fields in Northern Italy in the summer of 2016 (Table 1, Fig. 1, and the attached Google Earth file) with variable levels of common ragweed infestation. The fields where identified as having been used for cereal production (excluding maize). We visited the fields in August, visually estimated which percentage of the field was infested by common ragweed and recorded the visual impact of *Ophraella communa*.

2.3. Data

All 291 Level 1C images that partly or fully cover the two tiles (T32TMR and T32TLQ, Fig. 1) during 2016 were downloaded without further preprocessing (Drusch et al., 2012). Detailed RGB-images were

Table 1
Overview of field sites.

Nr	Name	Size (m^2)	Description situation 2016
1	Robecco sul Naviglio	49,365	Very heavily infested with common ragweed, no other vegetation, common ragweed completely destroyed by *Ophraella* by 25 August
2	Magnago	9899	High infestation of common ragweed among other vegetation, common ragweed completely destroyed by *Ophraella* by 25 August
3	Bienate	14,138	High infestation of common ragweed dominating the vegetation, common ragweed completely destroyed by *Ophraella* by 25 August
4	Magenta	9179	Some infestation of common ragweed, making up about half of the vegetation common ragweed completely destroyed by *Ophraella* after 25 August
5	Volvera	16,420	Medium infestation of common ragweed, attacked by Ophraella but period of destruction unknown

produced from band 4, 3 and 2 from the Sentinel-2 satellite by selecting a 1000 m circle of the image around the selected field. This allowed to visually assess if the field was influenced by e.g. clouds or shadows and at the same time allowed a visual assessment of the vegetation cover on the field.

2.4. Remote sensing data and cropping practice mapping

Before we calculated vegetation indices from the images, we removed clouds and other artefacts from the images using the accompanying mask files for each image. We selected the pixels corresponding to each of the five case study fields. Following the approach of e.g. Chen et al. (2014), Estel et al. (2016), Nguyen et al. (2012), Zhang and Hepner (2017), we calculated the NDVI value for each pixel (corresponding to 10 m × 10 m), since the geometric accuracy is at subpixel level (Clerc and MPC Team, 2017). For the analysis of the case study fields, data points influenced by clouds and shadows that had not been removed by the accompanying cloud mask were removed manually based on a visual inspection of the RGB-images. For each of the five fields, we subsequently plotted and visually analysed the time series based on the knowledge from the in situ observations of the fields along with the corresponding RGB images.

In order to map the cropping practice in the two Sentinel tiles (totalling $2.38 \cdot 10^8$ pixels) the area classified as "non-irrigated arable land" from Corine Land Cover (Bossard et al., 1994) was selected from the images and the NDVI time series for each pixel was calculated. This yielded approximately 35 million time series. Given the limited amount of training data in the present study, we have used unsupervised classification using similar principles as De Alwis et al. (2007) and Langley et al. (2001). Due to the large number of time series, the classification had to be done using the K-means procedure from Intel Data Analytics Abstraction Library (DAAL) (https://software.intel.com/en-us/intel-daal). The clustering procedure was applied in two steps.

(1) All 35 million time series were classified into six clusters. This number was determined, following the approach of Estel et al. (2016), by calculating the Davies-Bouldin index (Davies and Bouldin, 1979) for 2–40 clusters where six clusters had one of the lowest values. We labelled the classes based on plots of the cluster centroid time series compared with the classified map overlaid on WorldView 2 RGB images obtained from DigitalGlobe. The three general classes (fields, broadleaved trees and non-vegetation) could easily be determined from the WorldView 2 images, and the field data was used to further subclassify the pixels classified as fields. The visual inspection of the resulting map showed that field # 1, 2, 3 and 5 were in a class dominated by fields, whereas field #4 was classified in another class dominated by non-vegetation pixels. Apart from fields with training data and non-vegetation, three classes represented fields where no training data was available for the present study these were labelled as unclassified fields.
(2) To separate field #4 from the non-vegetation pixels, this class was further subdivided using the k-means clustering algorithm. Since these time series cover an approximately continuous region in NDVI, using the Davies-Bouldin index again yielded no useful results. By gradually increasing the number of clusters it was evident that 10 clusters were needed to separate field #4 and similar fields from the non-vegetation pixels. The remaining 9 classes, where we had no training data was then added to the class of unclassified fields or to the non-vegetation class based on a visual inspection of the classification overlaid on the WorldView-2 images. Similarly, the class with field #1, 2, 3 and 5 were divided into three subclasses using the k-means clustering, with the results representing gradually increased weed infestation, which could easily be interpreted from the plot of the cluster centroids and supported by the field observations.

2.5. Accuracy assessment

The accuracy assessment follows the procedure described in a concurrent study by some of the authors (Ottosen et al., in preparartion). Due to the limited amount of ground truth data in the present study, the accuracy assessment was done using Google Earth using similar procedures as e.g. Benza et al. (2016), Wickham et al. (2017), where ground truth is visually assessed from Google Earth. As the cropping practice is not directly detectable from Google Earth, only the land-use classification (fields, broadleaved trees, non-vegetation) was used similarly to the approach of Zhang et al. (2008). A stratified random sampling of 100 points in each land use class was used for the classification following the recommendation of Stehman (2001). The results were reported in the form of a confusion matrix including the user's and producer's accuracy (Congalton and Green, 2009).

3. Results and discussion

3.1. NDVI patterns in case study fields

The NDVI time series for the five case study fields are shown in Fig. 2. All five cases show a distinct phenological peak related to crop growth. Robecco sul Naviglio (Fig. 2a), Magnago via Trieste (Fig. 2b), Bienate (Fig. 2c) and Volvera (Fig. 2e) show a peak NDVI value around 1 May and a harvest date before 1 July, which indicates that these fields are winter crops. This interpretation is supported by Eurostat which states that wheat is very common and, according to Leff et al. (2004), wheat is mainly grown as a winter crop in Europe. Due to cloud cover in June 2016, it is not possible to determine the harvest date with greater precision. Magenta (Fig. 2d) shows a different pattern, with the field being practically bare until 1 May, hereafter the field turns green rapidly with a harvest date between 21 July and 10 August. This indicates that this field is an example of a spring crop, which according to Eurostat, is likely barley in this region. In summary, this means that the temporal resolution of Sentinel-2 is on the limit of being high enough for detecting the phenological characteristics of crop growth in this type of fields. It is evident that one or two cloud-covered images makes it difficult to detect features such as harvest date for single fields. Repeating the analysis after the launch of Sentinel-2B will yield a higher temporal resolution, which may alleviate this problem.

With respect to weed growth, in this case common ragweed, it can be seen that Robecco sul Naviglio shows a distinct peak NDVI value after the cropping season. Magnago via Trieste and Bienate show smaller peaks in the common ragweed growth season corresponding

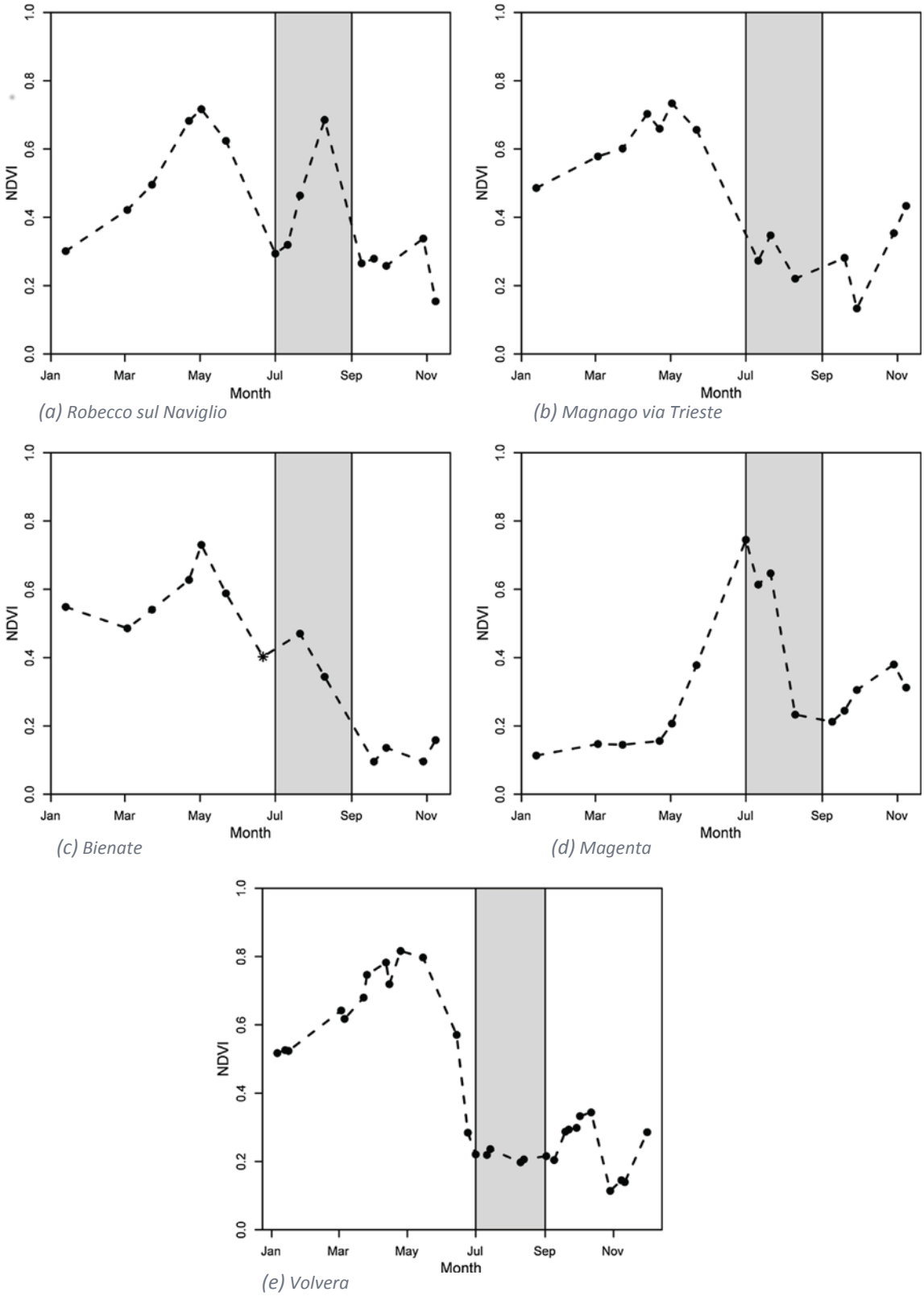

Fig. 2. Time series plots of the median value of NDVI for the five test sites. Spikes caused by clouds/shadows that have not been removed by the mask have subsequently been removed manually. The grey shaded area indicates roughly the period from wheat harvest (and appearing visibility of common ragweed plants) until the disappearance of common ragweed. The data point for 21 June for Bienate is marked with an asterisk since the image is influenced by a thin cloud cover.

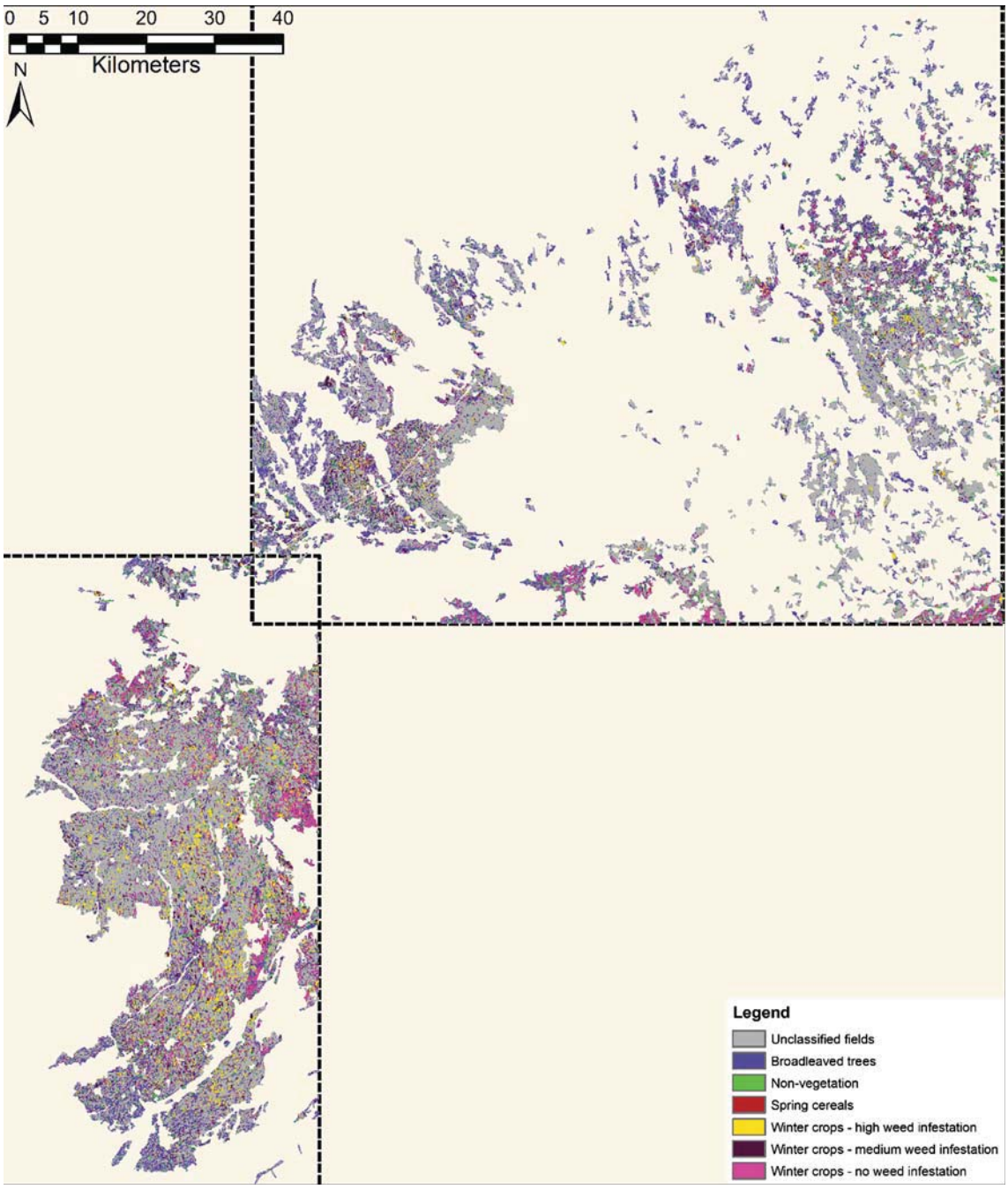

Fig. 3. Map of cropping practice for the two Sentinel-2 tiles.

Table 2
Area covered by the different classes. The percentages are of total agricultural land (total area minus non-vegetation and broadleaved trees (2769 km^2). The numbers from Eurostat are shown for comparison and corresponds to the region of Piedmont.

Class	Area (km^2)	Percentage (%)	Percentage Eurostat (%)
Unclassified fields	2136	77.1	71
Broadleaved trees	604		
Non-vegetation	202		
Spring cereal (excl. maize)	15	0.5	
Winter crops, – high weed infestation	164	5.9	
Winter crops – medium weed infestation	251	9.1	
Winter crops – no weed infestation	203	7.3	
Total winter crops	618	22.3	26
Other (e.g. durum wheat and oats)			3
Total	3575		

Table 3
Confusion matrix for the comparison between the land-use map and reference data generated from Google Earth including total accuracy (Total), user's accuracy (User), producer's accuracy (Prod) and number of pixels in each class (N).

Reference	Map Fields	Broadleaved	Non-vegetation	Total:	Prod:	N
Fields	31.3	18.7	6.0	56.0	56.0	168
Broadleaved	1.3	11.3	0.7	13.3	85.0	40
Non-Vegetation	0.7	3.3	26.7	30.7	87.0	92
Total	33.3	33.3	33.3	100.0		
User	94.0	34.0	80.0			
N	100	100	100			300

with the lower infestation levels observed in the field. From the RGB images for these two fields it can be seen, that although large parts of the fields are infested with weeds – in this case common ragweed – the density is not very high, which yields smaller peaks in the NDVI curves. Since the fields are reasonably homogeneous, dividing the fields into smaller areas would yield similar results. The pattern in Magenta is in line with the hypothesis that this land had been cropped with a spring crop, in which common ragweed will grow simultaneously with the crop. The second small peak in August may represent the regrowth of common ragweed after harvest (as observed on the ground), but could also be caused by the crop itself. For Volvera, the infestation level has probably been below the detection limit. In summary, this shows that weeds, in this case common ragweed, that grows on fields after harvest can be detected from NDVI time series from Sentinel-2, if present in sufficiently high densities. It is evident from Fig. 2 that the spatial resolution of Sentinel-2 is high enough to detect high weed infestations, whereas it is less applicable to lower infestation levels.

3.2. Mapping cropping practice

The map of the cropping practice of the region is shown in Fig. 3 and the area covered by the different classes is tabulated in Table 2. The table shows that 77% of the investigated area is agricultural land while 22% is non-agricultural areas. It is evident that the region is dominated by fields with a different phenology compared to the case studies. It is likewise evident that only a small fraction of the area shows the phenological signal of spring crops. Villa et al. (2015) clearly demonstrates that the spring crop maize has a very different phenological signal compared to the spring crops observed in our study. This suggest that the observed spring crops are mainly barley and our results of only 15 km^2 correspond well with the fact that only 1% of the area is used for barley (both winter and spring barley).

22% of the entire crop area has a phenological signal that corresponds to winter crops. This matches very well the data from Eurostat as about 26% of all cereals can be expected to be common wheat, hence winter crops, within this geographical region. Of these, approximately two thirds show some degree of weed infestation which must be considered a high number. The fact that the region is heavily infested with common ragweed means that a large part of this will be common ragweed. It is evident from Fig. 3 that especially the south-western part of the region is influenced by fields with high weed infestation. In this way, an increased understanding of the cropping practice, including the level of weed infestation, has been achieved for this region.

Assuming that the selection process using Corine Land Cover does not select most regions covered with rice, permanent crops and grassland, then the regions we have studied will be, according to Eurostat, mainly covered by cereals. This suggests that the unclassified field section in Table 2 is mainly maize as this is the majority of the crop that is not considered a winter crop.

The fact that seven phenological classes has been distinguished in Fig. 3, shows the potential for mapping cropping practice using Sentinel-2. With a spatial resolution of 10 m × 10 m, the present map has a higher spatial resolution compared to previous maps of cropping practice.

3.3. Accuracy assessment

The results of the accuracy assessment of the land-use map are shown in Table 3. The overall accuracy for all three land-use classes (correctly classified points divided by total number of points) is 69%. It is evident from Table 3 that the thematic accuracy for fields and non-vegetation are much higher than for broadleaved trees, which explains the slightly low overall accuracy. As can be seen, the number of broadleaved trees is overestimated and the confusion is mainly with fields. The reason is that certain fields show a phenological signal strongly resembling broadleaved trees. Samples from this type of fields were not collected for the present study, and future work should aim at distinguishing these. Given the high thematic accuracy of fields and non-vegetation, it is however the authors opinion that the results presented in the section on mapping of cropping practice are still valid.

4. Conclusions

Sentinel-2A is to some extent applicable for mapping cropping practice. The high spatial resolution of this satellite means that small and patchy elements, such as weed infestation, can be mapped in specific situations, where densities are sufficiently high. This shows the advantage of using a time series approach for the detection of weeds, in this case common ragweed. The temporal resolution of this satellite is high enough to detect some phenological features (growth of plants, harvest, weed growth and destruction by the *Ophraella communa*), however not high enough to detect other phenological elements such as harvest date, due to the presence of cloud cover in that period.

A more detailed understanding, as well as a map, of the cropping practice in Northern Italy has been obtained through the present study. This demonstrates that reasonable accurate maps of cropping practice can be produced from Sentinel-2A time series.

One remaining question is whether a better map of the cropping practice, including low ragweed infestations, could be obtained in situations with a lower cloud cover. It is also possible that a better map could be achieved after the launch of Sentinel-2B, which would increase the temporal resolution of the satellite to approximately 5 days or through using a combination of Sentinel-1, which is not influenced by cloud cover, and Sentinel-2.

Acknowledgements

We are thankful for contributed observations in the field by Benno Augustinus and Francesco Vidotto, and for discussions on the phenology of weeds with Francesco Vidotto, Gerhard Karrer, and Bruno Chauvel. We acknowledge financial support from the Swiss State Secretariat for Education, Research and Innovation (C13.0146), the COST Action FA1203 'Sustainable management of Ambrosia artemisiifolia in Europe (SMARTER)', and the project "New approaches for the early detection of tree health pests and pathogens" funded by BBSRC (ProjectID: BB/L012286/1)

Appendix A. Supplementary material

Supplementary data to this article can be found online at https://doi.org/10.1016/j.compag.2018.12.031.

References

Auda, Y., Déchamp, C., Dedieu, G., Blasco, F., Duisit, D., Pontier, E.J.L., 2008a. Détection des plantes envahissantes par télédétection : un cas d'étude, l'ambroisie en région Rhône-Alpes, France. Int. J. Remote Sens. 29, 1109–1124.

Auda, Y., Hagolle, O., Gastellu-Etchegorry, J.-P., Rakotoniaina, S., Roux, R., Meon, H., Dechamp, C., 2008b. Contribution of multi-temporal very high resolution images to Ambrosia Artemisiifolia L. remote sensing. Allergo J. 17, 380.
Bégué, A., Arvor, D., Bellon, B., Betbeder, J., de Abelleyra, D.P.D., Ferraz, R., Lebourgeois, V., Lelong, C., Simões, M., Verón, R., S., 2018. Remote sensing and cropping practices: a review. Remote Sens. 10.
Benza, M., Weeks, J.R., Stow, D.A., López-Carr, D., Clarke, K.C., 2016. A pattern-based definition of urban context using remote sensing and GIS. Remote Sens. Environ. 183, 250–264.
Bossard, M., Feranec, J. & Otahel, J., 1994. CORINE Land Cover. Technical Guide.
Chen, L., Jin, Z., Michishita, R., Cai, J., Yue, T., Chen, B., Xu, B., 2014. Dynamic monitoring of wetland cover changes using time-series remote sensing imagery. Ecol. Inf. 24, 17–26.
Ciappetta, S., Ghiani, A., Gilardelli, F., Bonini, M., Citterio, S., Gentili, R., 2016. Invasion of Ambrosia artemisiifolia in Italy: Assessment via analysis of genetic variability and herbarium data. Flora – Morphol., Distrib., Functional Ecol. Plants 223, 106–113.
Clerc, S., & MPC Team, 2017. Sentinel 2 Data Quality Report.
Congalton, R.G., Green, K., 2009. Assessing the Accuracy of Remotely Sensed Data: Principles and Practices. CRC Press/Taylor & Francis.
Davies, D.L., Bouldin, D.W., 1979. A cluster separation measure. IEEE Trans. Pattern Anal. Mach. Intell., PAMI-1, pp. 224–227.
de Alwis, D.A., Easton, Z.M., Dahlke, H.E., Philpot, W.D., Steenhuis, T.S., 2007. Unsupervised classification of saturated areas using a time series of remotely sensed images. Hydrol. Earth Syst. Sci. 11, 1609–1620.
Drusch, M., del Bello, U., Carlier, S., Colin, O., Fernandez, V., Gascon, F., Hoersch, B., Isola, C., Laberinti, P., Martimort, P., Meygret, A., Spoto, F., Sy, O., Marchese, F., Bargellini, P., 2012. Sentinel-2: ESA's optical high-resolution mission for GMES operational services. Remote Sens. Environ. 120, 25–36.
Estel, S., Kuemmerle, T., Levers, C., Baumann, M., Hostert, P., 2016. Mapping cropland-use intensity across Europe using MODIS NDVI time series. Environ. Res. Lett. 11 024015–024015.
Harris, I., Jones, P.D., Osborn, T.J., Lister, D.H., 2014. Updated high-resolution grids of monthly climatic observations - the CRU TS3.10 Dataset. Int. J. Climatol. 34, 623–642.
Jakubauskas, M.E., Legates, D.R., Kastens, J.H., 2002. Crop identification using harmonic analysis of time-series AVHRR NDVI data. Comput. Electron. Agric. 37, 127–139.
Kazinczi, G., Béres, I., Novák, R., Bíro, K., Pathy, Z., 2008. Common ragweed Ambrosia artemisiifolia: a review with special regards to the results in Hungary. I. Taxonomy, origin and distribution, morphology, life cycle and reproduction strategy. Herbologia 9, 55–91.
Laba, M., Tsai, F., Ogurcak, D., Smith, S., Richmond, M.E., 2005. Field determination of optimal dates for the discrimination of invasive wetland plant species using derivative spectral analysis. Photogramm. Eng. Remote Sens. 71, 603–611.
Langley, S.K., Cheshireb, H.M., Humes, K.S., 2001. A comparison of single date and multitemporal satellite image classifications in a semi-arid grassland. J. Arid Environ. 49, 401–411.
Latombe, G., Pyšek, P., Jeschke, J.M., Blackburn, T.M., Bacher, S., Capinha, C., Costello, M.J., Fernández, M., Gregory, R.D., Hobern, D., Hui, C., Jetz, W., Kumschick, S., McGrannachan, C., Pergl, J., Roy, H.E., Scalera, R., Squires, Z.E., Wilson, J.R.U., Winter, M., Genovesi, P., McGeoch, M.A., 2017. A vision for global monitoring of biological invasions. Biol. Conserv. 213, 295–308.
Leff, B., Ramankutty, N., Foley, J.A., 2004. Geographic distribution of major crops across the world. Global Biogeochem. Cycles 18, 18.
Lehoczky, É., Buszynák, J., Gólya, G., 2013. Study on the spread, biomass production, and nutrient content of ragweed with high-precision GNSS and GIS device system. Commun. Soil Sci. Plant Anal. 44, 535–545.
Müller-Schärer, H., Lommen, S.T.E., Rossinelli, M., Bonini, M., Boriani, M., Bosio, G., Schaffner, U., Hatcher, P., 2014. Ophraella communa, the ragweed leaf beetle, has successfully landed in Europe: fortunate coincidence or threat? Weed Res. 54, 109–119.
Müllerová, J., Brůna, J., Bartaloš, T., Dvořák, P., Vítková, M., Pyšek, P., 2017. Timing is important: unmanned aircraft vs. satellite imagery in plant invasion monitoring. Front. Plant Sci. 8, 1–13.
Ngom, R., Gosselin, P., 2014. Development of a remote sensing-based method to map likelihood of common ragweed (ambrosia artemisiifolia) presence in urban areas. IEEE J. Sel. Top. Appl. Earth Obs. Remote Sens. 7, 126–139.
Nguyen, T.T.H., de Bie, C.A.J.M., Ali, A., Smaling, E.M.A., Chu, T.H., 2012. Mapping the irrigated rice cropping patterns of the Mekong delta, Vietnam, through hyper-temporal SPOT NDVI image analysis. Int. J. Remote Sens. 33, 415–434.
Oerke, E.C., 2006. Crop losses to pests. J. Agric. Sci. 144, 31–43.
Olsen, O., 2010. Agriculture and fisheries A regional picture of farming in Europe — what, where and how much? Eurostat Statistics in focus.
Ottosen, T.-B., Petch, G., Hanson, M., Skjøth, C. Accuracy assessment of high resolution maps of European conifer and broadleaved trees based on Sentinel-2. Remote Sensing of Environment (in preparation).
Rakotoniaina, S., Auda, Y., Blasco, F., Déchamp, C., 2009. Comparaison Des Méthodes de Classification Non Paramétrique (k-NN) et Contextuelle (ICM) Appliquées à La Cartographie Par Télédétection Du Niveau d ' Infestation Par l ' Ambroisie Comparison of the k-NN Nonparametric and the ICM Contextual Classification Methods Applied to the Remote Sensing Detection of Ragweed. Ambroisie, First Int. Ragweed Rev. 26, 77–87.
Smith, M., Cecchi, L., Skjøth, C.A., Karrer, G., Šikoparija, B., 2013. Common ragweed: A threat to environmental health in Europe. Environ. Int. 61, 115–126.
Sölter, U., Mathiassen, S., Verschwele, A., 2016. Combining cutting and herbicide application for Ambrosia artemisiifolia control. In: 27th German Conference on Weed Biology and Weed Control.
Stehman, S.V., 2001. Statistical rigor and practical utility in thematic map accuracy assessment. Photogramm. Eng. Remote Sens. 67, 727–734.
Villa, P., Stroppiana, D., Fontanelli, G., Azar, R., Brivio, P., 2015. In-season mapping of crop type with optical and X-band SAR data: a classification tree approach using synoptic seasonal features. Remote Sens. 7, 12859–12886.
Wickham, J., Stehman, S.V., Gass, L., Dewitz, J.A., Sorenson, D.G., Granneman, B.J., Poss, R.V., Baer, L.A., 2017. Thematic accuracy assessment of the 2011 National Land Cover Database (NLCD). Remote Sens. Environ. 191, 328–341.
Zhang, X., Sun, R., Zhang, B., Tong, Q., 2008. Land cover classification of the North China Plain using MODIS_EVI time series. ISPRS J. Photogramm. Remote Sens. 63, 476–484.
Zhang, Y., Hepner, G.F., 2017. The Dynamic-Time-Warping-based k-means+ + clustering and its application in phenoregion delineation. Int. J. Remote Sens. 38, 1720–1736.